Journal of Structural Geology 31 (2009) 575–581

Contents lists available at ScienceDirect

Journal of Structural Geology

journal homepage: www.elsevier.com/locate/jsg

Analysis of complete fold shape based on quadratic Bézier curves☆

Chun Liu*, Yikun Zhang, Yuan Wang

School of Earth Sciences and Engineering, Nanjing University, 22 Hankou Road, Nanjing 210093, China

ARTICLE INFO

Article history:
Received 10 May 2008
Received in revised form
19 February 2009
Accepted 17 March 2009
Available online 15 April 2009

Keywords:
Fold shape
Bézier curve
Fold classification
Quantitative description

ABSTRACT

Six segments of quadratic Bézier curve are joined together according to some geometrical rules to approximate fold shape. In a classification of folds based on this method, an ideal fold shape is determined by two parameters. The first one, u_c, termed the axial lift-up ratio of the central part, generates the folds within a broad spectrum of forms ranging from box folds to chevron folds. The other one, γ, is the interlimb angle. In the quantitative description of complete folds with multiple layers, three new parameters, θ, T and E are used to describe the deflection angle of the axial plane, the thickness increment of hinge zone and the limb elongation, respectively. Based on the modeling method, the program "Bézier Fold Profiler" has been developed, with which most types of folds can be simulated by varying thirteen parameters. Two description methods, complete fold description and individual layer description, can be used for the quantitative analysis of folds. The description methods are carried out by the visual matching of the fold profile displayed on-screen from an imported digital image. The layer curves of the model are displayed on the fold image. This method has the advantage of speed and simplicity.

1. Introduction

Fold shapes control the location of some important mineral resources such as oil, gas and saddle-reef gold deposits. The precise description of the geometry of folds is in many cases the only tool available to analyze the origin and evolution of these structures. The research on geometry and kinematics of folding is ongoing, but still it does not satisfy the requirements demanded from real application.

There have already been numerous studies concerned with fold shape, in which a fold is approximated by a series of mathematical functions (Bastida et al., 2005). For example, Chapple (1968) and Stabler (1968) have used the Fourier analysis for the quantitative description of fold shapes, each limb being characterized by several coefficients of a Fourier sine series. However, the number of coefficients is too large and inconvenient for classification. Hudleston (1973) improved the method, using only two Fourier coefficients to classify the shape of folds, and distinguished 30 idealized fold forms for comparison with natural folds. Nevertheless, this method only gives a rough approximation to the function that describes fold. Other methods have employed other types of mathematical functions. Bastida et al. (1999) proposed a method to approach fold shapes using power functions. Their method is based on the use of two parameters: the exponent, n, describing the shape, and the amplitude/wavelength ratio. Aller et al. (2004) suggested that different fold shapes can be matched with portions of conics and distinguished on a graph of eccentricity and aspect ratio. Srivastava and Lisle (2004) used computer-aided Bézier curve analysis and reduced eight variables to only two variables for describing a fold. The first parameter, L, is related to the distribution of curvature on a single limb of a fold between the hinge point and the inflection point, and the other parameter, R, is related to the ratio of amplitude to wavelength. These studies have employed a number of different methods for classification and description of folds.

The aim of this paper is to present a geometrical analysis of fold profiles based on the approximation of fold geometries by six quadratic Bézier curves, which are joined together according to some geometrical rules. As in Srivastava and Lisle (2004), an ideal fold is described and classified using two parameters. The results can be plotted on a graph which reflects the main geometrical features of the fold profiles. However, the method of Srivastava and Lisle analyzes individual fold limbs; and the shape of a complete fold can hardly be determined by only two variables. Our new model extends the application of Bézier curves that can simulate a broader spectrum of complete fold shapes ranging from straight-limbed chevron folds, to rounded geometries, and even box folds. Further, three more parameters are used to describe complex fold shape. This paper offers a feasible method for fold classification and

☆ Information and software on the fold simulation developed in this paper are available in: http://www.acei.cn/program/folds.htm.

* Corresponding author. Tel.: +86 25 83686797; +86 25 83596220.
E-mail address: oxtown@gmail.com (C. Liu).

0191-8141/$ – see front matter © 2009 Elsevier Ltd. All rights reserved.
doi:10.1016/j.jsg.2009.03.019

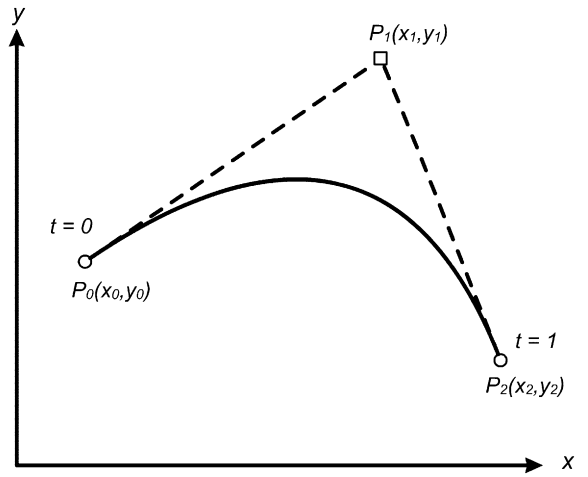

Fig. 1. A quadratic Bézier curve defined by three control points: P_0, P_1, P_2. The two lines P_0P_1 and P_2P_1 are the tangents at the points P_0 and P_2 respectively.

quantitative description, which can be used in further geometric and kinematic studies of folds (Liu et al., 2009).

2. Modeling and fold classification

The use of Bézier curves as a tool to describe curvatures and surfaces was introduced by French engineers of the automobile industry, in particular Bézier (1966, 1967). More recently, the concept was recognized as useful in geological description (De Paor, 1996) and used as a tool for fold shape analysis (Srivastava and Lisle, 2004) and flanking structures description (Coelho et al., 2005). Bézier curve has demonstrated its versatility for analyzing a wide range of fold geometries. However, several segments of curve should be joined to approximate the fold shape, since it is hard to describe a fold by only one curve defined by mathematic functions. In this paper, an individual folded layer is approximated by six segments of quadratic Bézier curve.

2.1. Quadratic Bézier curves

A quadratic Bézier curve is uniquely defined by the position of three points (Fig. 1): two points, $P_0(x_0, y_0)$ and $P_2(x_2, y_2)$ marking the two ends of the curve and one further control point, $P_1(x_1, y_1)$. The parametric equations of a segment of a quadratic Bézier curve are (Bézier, 1966, 1967):

$$x(t) = (1-t)^2x_0 + 2(1-t)tx_1 + t^2x_2 \quad (1a)$$

$$y(t) = (1-t)^2y_0 + 2(1-t)ty_1 + t^2y_2 \quad (1b)$$

The parameter t indicates positions along the Bézier curve from the start point P_0, where $t=0$, towards the end point P_2, where $t=1$. The Bézier curve, made up of a succession of points corresponding to different t values, is therefore defined by the coordinates of points P_0, P_1 and P_2. Since P_0P_1 and P_2P_1 are the tangent at the points P_0 and P_2 respectively, the quadratic Bézier curve can be determined by the two end points (P_0 and P_2) and the slope (k_0 and k_2) of the corresponding segments (P_0P_1 and P_2P_1). The two parameters, x_1 and y_1 (Eqs. (1)) can be replaced by the slopes:

$$x_1 = (k_0x_0 - k_2x_2 + y_2 - y_0)/(k_0 - k_2) \quad (2a)$$

$$y_1 = (k_0k_2x_0 - k_0k_2x_2 - k_2y_0 + k_0y_2)/(k_0 - k_2) \quad (2b)$$

2.2. Modeling of an ideal fold

The ideal fold is a symmetrical fold with rounded shape and constant orthogonal thickness. In this example of modeling, limb dips are $a_1 = 60°$ and $a_2 = 120°$. The folded layer is divided into three parts by two inflection points (points B and C in Fig. 2). Each part is approximated by two Bézier curves that are connected at the "hinge point" (such as point G in Fig. 2). Hence, each layer of the fold is approximated by six Bézier curves. The ideal fold can be drawn by the following steps:

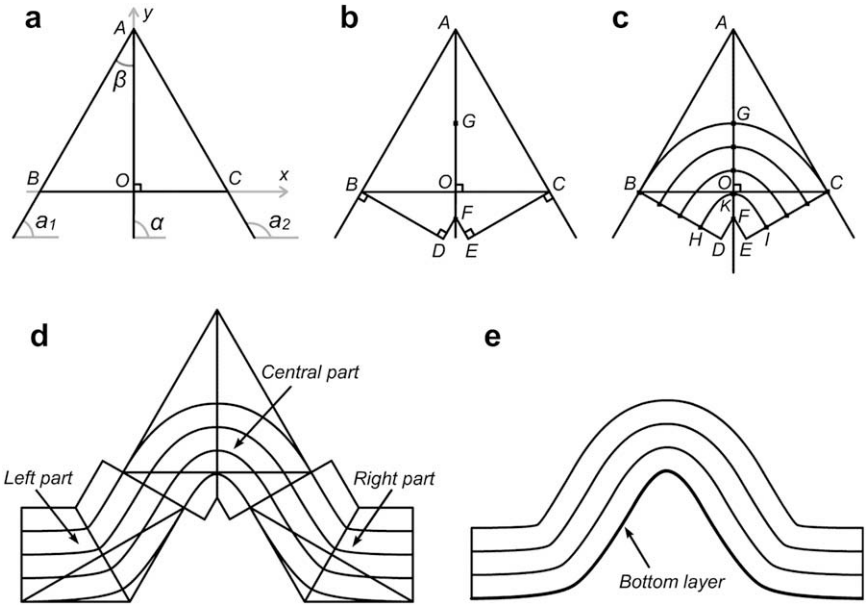

Fig. 2. Modeling of an ideal fold based on the connection of six quadratic Bézier curves. (a) Draw an isosceles triangle ABC; a_1 and a_2 represent the limb dips. (b) Points F and G are the core and the hinge of the fold, respectively; FG is the axial plane of the fold. (c) Find the control points of each bed on segments BD, FG and CE equidistantly. The central part can be drawn by connecting the end points with Bézier curves. (d) Two limbs are drawn according to the rules shown for the central part. (e) The final shape of the ideal fold.

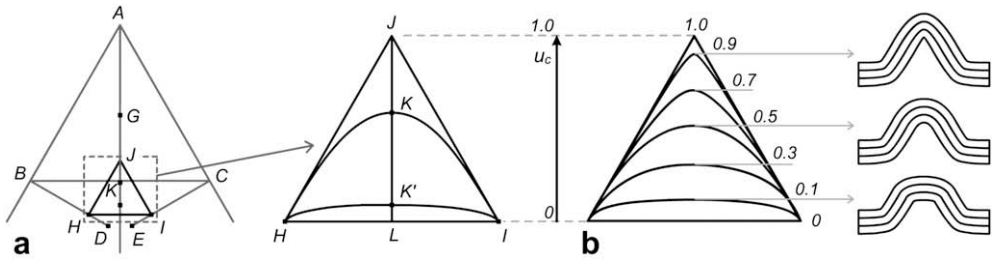

Fig. 3. (a) $u = l_{KL}/l_{JL}$, which represents axial lift-up ratio is used to describe the distribution of curvature between the hinge point and the inflection point. (b) A spectrum of fold forms with the uniform interlimb angle (60°) and various u values from 0 to 1.0, shows that the fold shape tends to be sharper with the increase of u.

(1) Confine the area of the fold. Draw an isosceles triangle *ABC*, in which the points *B* and *C* represent the inflection points on the fold limbs. *AB* and *AC* are the tangents of the folded layer at points *B* and *C*, respectively. The angles that *AB* and *AC* form with the *x* axis represent the limb dips (i.e. a_1 and a_2). The origin of coordinates is set at point *O*, with *AO* being the bisector line of $\angle BAC$. Hence, $BO = CO = w$, where w is a parameter that can be used to describe the fold size.

(2) Find the fold core. Draw *BD* and *CE* perpendicular to *AB* and *AC*, respectively, and let $BD = CE = w$. Then, draw perpendiculars to *BD* and *CE* in *D* and *E*, respectively. The two perpendiculars intersect at point *F*, which is defined as the fold core. Find another point *G* along the direction of *FA*, which makes $FG = w$. The point *G* and the segment *FG* are defined as the hinge point and the axial plane, respectively. The angle that the segment *FG* forms with the *x* axis is defined as the dip angle of the axial plane, which can be calculated from the following equation:

$$\alpha = (a_1 + a_2)/2 \tag{3}$$

Note that the triangle *ABC* is an isosceles triangle, points *F* and *G* should be on the line *AO*.

(3) Draw the central part. Mark the end points of each layer on segments *BD*, *FG* and *CE* equidistantly, and connect the corresponding end points with Bézier curves. For example, the points, *H*, *K* and I, are the end points of the bottom layer. Connect the corresponding end points with two Bézier curves, one Bézier curve with the end points *H* and *K* and the other *K* and I. Each of the two Bézier curves is drawn according to the position of its two end points and the slope at the end points in Eqs. (1) and (2). The common slope of the two Bézier curves at the hinge point *K*, where they are connected, is assumed to be perpendicular to the fold axial plane, while the slopes at the end points *H* and *I* are given as the dips of fold limbs (a_1 and a_2 respectively). As a result, the bottom layer is determined by the three parameters: *w*, which determines the size of fold, a_1 and a_2, which are the limb dips. Since the Bézier curve of other layers can also be drawn in a similar way, the central part of the anticline is defined by only three parameters.

(4) Draw the limbs. The left side of the left limb connects with horizontal strata, while the other side connects with the inflection point *B* and the corresponding segment *BD*. Similarly, the left side of the right limb connects with the inflection point *C* and the segment *CE*. Repeat steps (1)–(3) to draw the two limbs (Fig. 2d).

Remove all the assistant lines and points, Fig. 2e shows the final shape of the ideal fold, which is determined by only three parameters: *w*, a_1 and a_2.

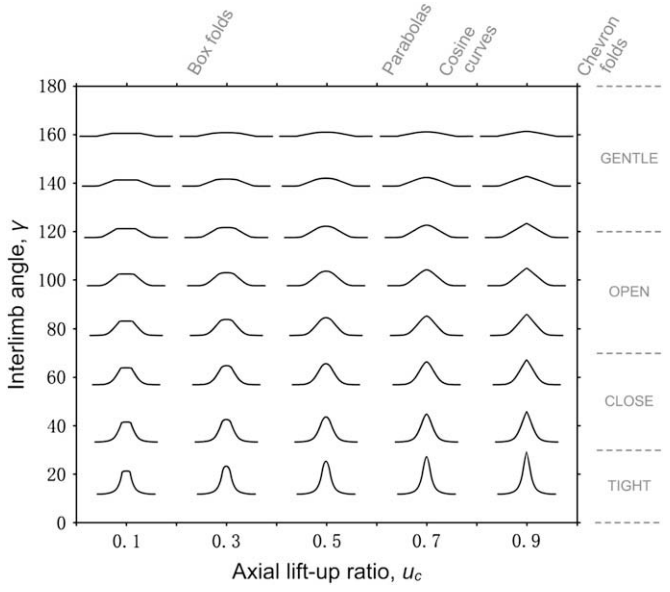

Fig. 4. Fold shapes defined by u_c and γ. Note that we use the bottom layer to represent a complete fold.

2.3. A method of fold classification

An ideal fold which approximates to a cosine curve shape has been drawn according to the basic modeling method described above. However, in order to simulate more types of folds, such as chevron folds and box folds, a new shape parameter is used to describe the curvature distribution of the fold. Note that the shape of the hinge zone is controlled by the position of *FG*. Move *FG* along the direction of *FG*, hinge zone will be sharper, changing from cosine curves to the chevron shape with the increase of displacement. Conversely, move *FG* in the opposite direction, and an approximation to box forms is obtained (Fig. 3b). Hence, a new parameter u, termed axial lift-up ratio, is used to describe the distribution of curvature between the hinge point and the inflection point:

$$u = l_{KL}/l_{JL} \tag{4}$$

where l_{KL} and l_{JL} represent the length of the line segments *KL* and *JL* in Fig. 3a, in which *H*, *K* and *I* are the three control points of the bottom layer (see also Fig. 2c); the point *J* is determined from the inflection points *H* and *I* and the dips of two fold limbs (*JH* and *JI* are parallel to *AB and AC*, respectively).

Sharpness of the left, central and right parts are determined by corresponding axial lift-up ratio respectively u_l, u_c and u_r. However, only u_c is used to distinguish fold shapes in the classification of ideal folds. The left and right parts are drawn following the method introduced in Section 2.2, which maintain an approximately

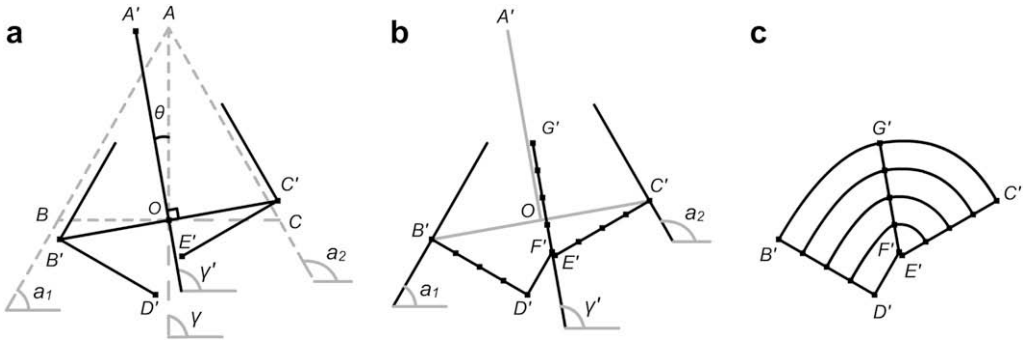

Fig. 5. (a) $\theta = \angle AOA'$, termed the deflection angle of the axial plane. (b–c) Anti-clockwise deflection of axial plane leads to the shortening of the right side.

uniform distribution of curvature. Fig. 3b shows how the shape parameter u_c controls the curvature distribution of folds.

As described above, the method defines an ideal fold based on four parameters, w, a_1, a_2 and u_c. Since it is impractical to classify folds based on four parameters, we will reduce four parameters to two parameters for describing the fold shape. A classical parameter used to describe the fold tightness is the interlimb angle (γ), which was used by Fleuty (1964) to differentiate the following types of folds: gentle ($180^\circ > \gamma > 120^\circ$), open ($120^\circ \geq \gamma > 70^\circ$), close ($70^\circ \geq \gamma > 30^\circ$), tight ($30^\circ \geq \gamma > 0^\circ$), isoclinal ($\gamma = 0^\circ$) and elasticas ($\gamma < 0^\circ$). Firstly, a_1 and a_2 change the fold shape by varying the interlimb angle, so we choose the interlimb angle γ to replace a_1 and a_2:

$$\gamma = a_2 - a_1 \tag{5}$$

Secondly, we assume $w = 1$, since the curve shape is not affected by the fold size.

As a result of these simplifications, the shape of an ideal fold is defined by only two parameters: u_c and γ. Fig. 4 shows how the two parameters control the fold shape. When $u_c = 0$, corresponds to box folds with curvature concentrated in two corners. On the other end, $u_c = 1$, corresponds to approximately chevron folds with straight limbs and curvature concentrated at the hinge. When $0 < u_c < 1$, with the intermediate forms appear that give a good fit of common fold shapes as box folds, cosine curves, parabolas and chevron folds. Along the vertical axis, four main types of folds are distinguished: gentle, open, close and tight. Unfortunately, isoclinal folds ($\gamma = 0$) are not included in this classification, since the definition equation of u (Eq. (4)) requires that the tangents (JH and JI in Fig. 3a) at two inflection points should intersect at one point (J in Fig. 3), whereas $\gamma = 0$ leads to parallel lines without intersection point.

3. Quantitative description of fold shape

An ideal fold is determined by two parameters u_c and γ. However, its impossible to describe a complex natural fold by only two parameters. Here, three more parameters are introduced to describe more types of folds, such as inclined folds, overturned folds etc.

3.1. Deflection angle of axial plane

A new parameter θ, which is termed deflection angle of the axial plane, is defined to make possible the fit of inclined folds. In Fig. 2, the axial plane FG (i.e. OA) is the symmetry axis of the fold. Deflection of the axial plane will lead to distortion of hinge zone, while limb dips and layer thickness are unchanged. Consequently, dip angle of the axial plane should be redefined as:

$$\alpha = (a_1 + a_2)/2 + \theta \tag{6}$$

In Fig. 5a, $\theta = \angle AOA'$, indicates the deflection angle of the axial plane, since the axial plane $F'G'$ is always parallel to $O'A'$. In Fig. 5b, $B'D'$ and $C'E'$ are still perpendicular to AB and AC, respectively; the perpendiculars of $B'D'$ and $C'E'$ intersect at point F'; and Bézier curves are drawn according to the rules presented in Section 2.2. Application of parameter θ enables the description of inclined folds in this model (Fig. 7a).

3.2. Thickness increment of the hinge zone

Layer thickness changes are common in natural folds, especially in the fold hinge area.

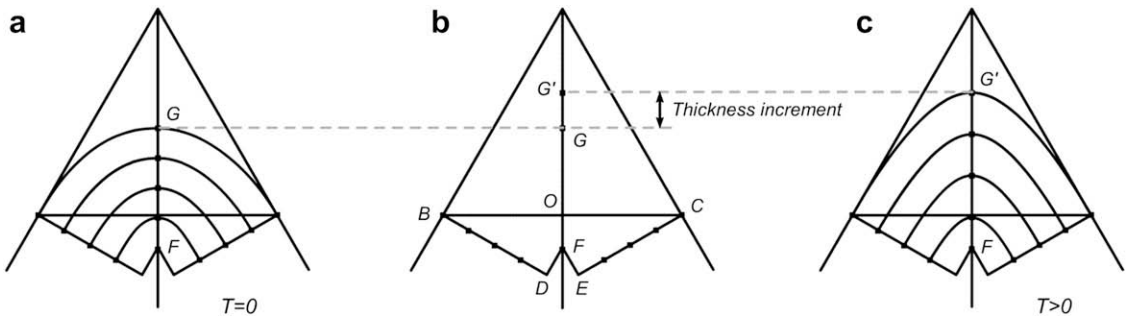

Fig. 6. Thickness increment of the hinge zone: $T = (FG - w)/w$. (a) $T = 0$, corresponds to constant orthogonal thickness. (b–c) When $T > 0$, the hinge point is moved to the position G' to change the layer thickness of the hinge zone.

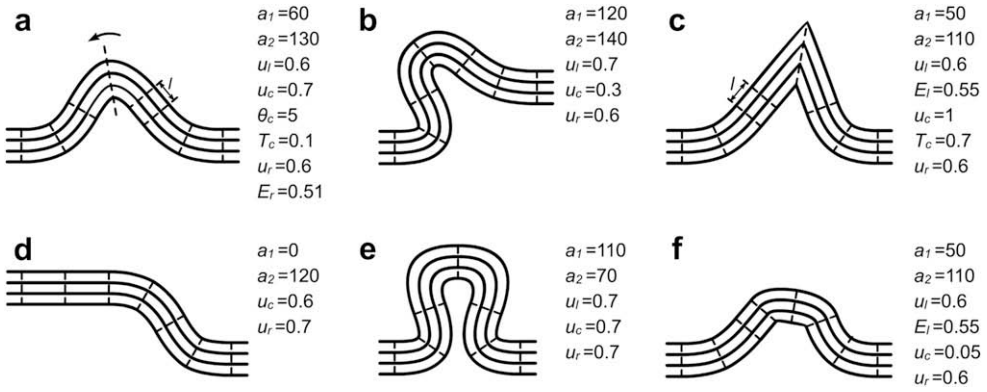

Fig. 7. Various fold forms controlled by the parameters listed to the right. (a) Inclined fold, (b) Overturned fold. (c) Chevron fold. (d) Monocline. (e) Fan fold. (f) Box fold. Note that parameters which equal to zero are not shown.

Therefore, another parameter T is introduced to describe the thickness increment of the hinge zone, which is defined as:

$$T = (l_{FG} - w)/w \tag{7}$$

where l_{FG} represents the length of segment FG in Fig. 6b, and w is the parameter mentioned above, which has been used to describe the fold size. Fig. 6 illustrates how the parameter T controls the layer thickness. When $T = 0$, the layer thickness is constant. When $T > 0$, point G moves along the FG direction, as a result, segment FG is extended. Consequently, all layers in the fold hinge area tend to be thicker, while the layer thickness at the inflection points remains constant (Fig. 6c). Conversely, when $T < 0$, all layers in fold hinge area tend to be thinner.

3.3. Limb elongation

In Fig. 7a and c, the fold limb is extended for a distance l, which makes possible to set the two limbs on the same level. Limb elongation (E) is expressed as:

$$E = l/w \tag{8}$$

Fig. 7a shows that the anti-clockwise deflection of the axial plane leads to a small shortening of the right side (see also Fig. 5c). And in Fig. 7c, since the right limb is steeper than the left limb, in order to keep two limbs at the same level, the left part is moved for a certain distance along the dip direction. The parameter E controls the length of limbs and the vertical position of the corresponding horizontal layers.

As a result, the shape of a fold is determined by the thirteen parameters: a_1, a_2, u_l, θ_l, T_l, u_c, θ_c, T_c, u_r, θ_r, T_r, E_l and E_r. The subscripts, l, c and r, represent the parameters of left part, central part and right part, respectively. Note that the interlimb angle (γ) is not used in the quantitative description, as it can be calculated from Eq. (5).

4. The program "Bézier Fold Profiler"

The complexity of the model presented in this paper makes it impractical to draw a fold by manual drawing. Inspired by the method based on modeling curves using dedicated drafting software (Srivastava and Lisle, 2004) and a MatLab program for fold classification (Lisle et al., 2006), this section describes a program for fold classification and quantitative description, based on the on-screen matching of an imported image of the fold with mathematically defined Bézier curves. The program, "Bézier Fold Profiler", is a Flash program running in the web (see the article footnote for additional information of the program), in which the curves are remodeled, by changing their parameters until a close fit is obtained.

By using "Bézier Fold Profiler", a natural fold can be approximated according to the procedure below: (1) Import the digital image of the fold into the program. Adjust the size of the image

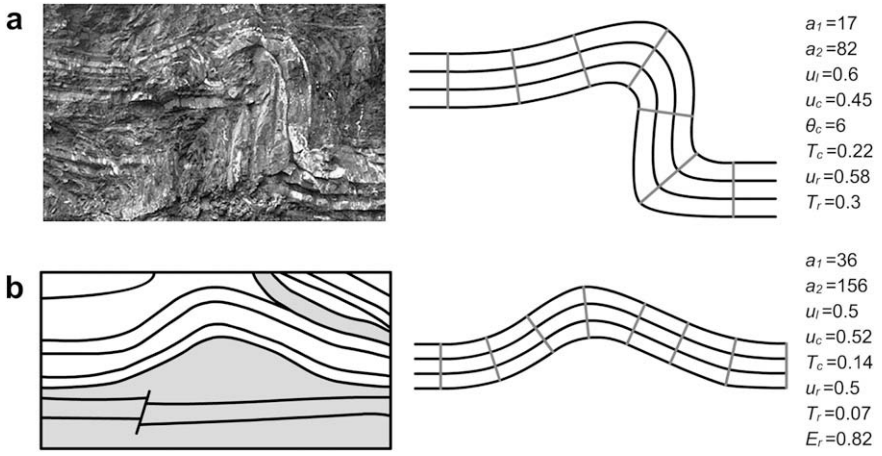

Fig. 8. The complete fold description method applied to two examples. (a) A drag fold associated with a thrust fault, Gaspe Peninsula, Canada. (b) A detachment fold, Tarim Basin, Xinjiang province, China.

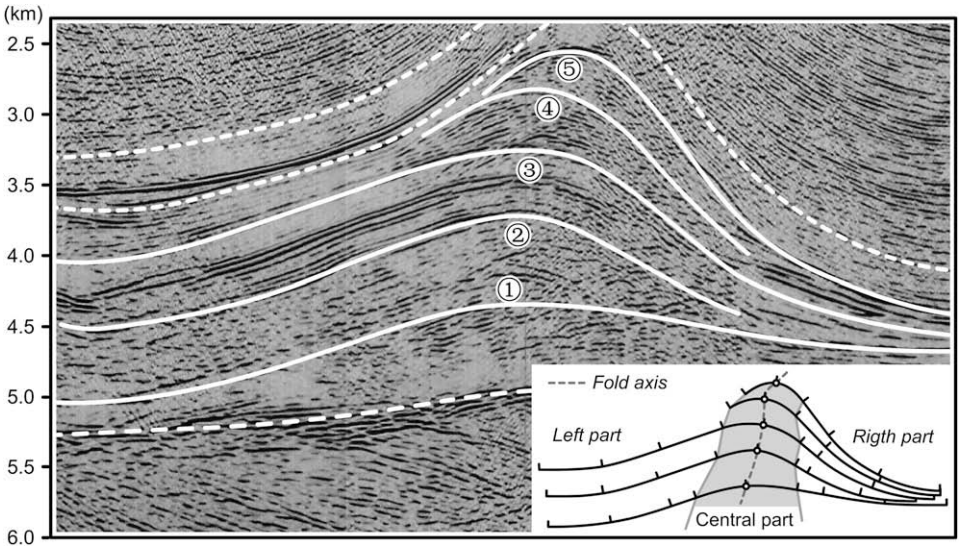

Fig. 9. The individual layer description method applied to analyze the seismic section of Kuqa foreland fold-and-thrust belt, Xinjiang, China.

until the layer thickness of the fold equals the default thickness. (2) Set the limb dips (a_1 and a_2), limb elongation (E) and the axial lift-up ratio (u), according to the shape of the natural fold. (3) Change T if it is necessary. (4) Adjust the deflection angle of the axial plane (θ) and E until the program traces out the natural fold shape.

In general, box folds are difficult to simulate by Bézier curves because of the lack of inflection points between successive hinges (Srivastava and Lisle, 2004). However, in the new model, an individual folded layer is approximated by six segments of Bézier curve and a broad spectrum of fold shapes ranging from box forms to chevron forms can be simulated. Fig. 7 illustrates some general forms of folds, which are determined by the right-hand description parameters. Comparing Fig. 7c with Fig. 7f, we see that the main difference between the chevron fold and the box fold lies in the different axial lift-up ratio of the central part (u_c). Fig. 7d shows that monoclines can be regarded as folds with a zero dip angle in one limb. Furthermore, fan folds with a negative interlimb angle could also be simulated by varying limb dips (Fig. 7e).

5. Description methods and examples

In the program, a fold can be analyzed by two description methods: complete fold description and individual layer description. For the purpose of illustration of the new methods, we present three examples here.

Table 1
Quantitative analysis data of the five layers of Fig. 9.

No.	a_1	a_2	u_l	u_c	u_r	E_l	E_r	γ
①	19°	170°	0.58	0.58	0.75	0.42	0.42	151°
②	19°	150°	0.65	0.62	0.6	1.1	0.25	131°
③	19°	140°	0.7	0.47	0.45	1.05	0.36	121°
④	32°	134°	–	0.48	0.4	–	0.7	102°
⑤	38°	127°	–	0.5	0.4	–	0.68	89°

5.1. Complete fold description

This description method analyzes the complete fold by varying thirteen parameters according to the procedure introduced in Section 4. In this method, the two parameters θ and T are included, which indicate the relationships between layers. Variation of θ changes the position of the hinge points in each layer, and consequently changes the distribution of curvature between hinge points and deflection points. With the increase of T, the shape of the upper layers becomes sharper, while the bottom layer is unchanged (Fig. 7c). Hence, the parameter T indicates the variation of curvature distribution between layers.

Fig. 8a shows a natural drag fold in which the dip angle of the left limb is small, whereas the right limb is nearly vertical, defining a shape similar to that of Fig. 7b. The layer thickness at the hinge zone is greater than that of the two limbs, i.e. $T_c > 0$. Simulation results are shown in the right-hand side of Fig. 8a. The couple of data $u_c = 0.45$ and $\gamma = 65°$ correspond to the parabola shape in the classification.

The second example (Fig. 8b) is a seismic interpretation map of a detachment fold. Changes of thickness are small along the folded layer, which indicates a small T. Since the slope of the left limb is greater, right limb should be extended to keep the two limbs on the same level. The simulation results are shown in the right-hand side of Fig. 8b, which gives a good fit of the natural fold. The couple of data $u_c = 0.52$ and $\gamma = 120°$ correspond to the parabola shape in the u_c–γ graph.

5.2. Individual layer description

The complete fold description method is unsuitable for those irregular fold forms with high deformation, such as cases of uneven changes of layer thickness or curvilinear axial plane. The individual layer description method is introduced to deal with these situations. In this method, each bed of a natural fold is approximated by the bottom layer (Fig. 2e) of the default fold in the program, and consequently determined by a series of shape parameters. The shape of the bottom layer is not affected by the parameter T, which can be ignored in this method. Furthermore, we assume $\theta = 0$, as the bottom curves almost remain unchanged when θ increases. Therefore, each folded layer is determined by seven parameters: a_1, a_2, u_l, u_c, u_r, E_l and E_r.

Fig. 9 is a seismic section map of Kuqa foreland fold-and-thrust belt, Xinjiang, China. The individual layer description method was used to analyze the five layers which have been drawn on this cross-section. The parameters of these layers are listed in Table 1, which show that the interlimb angle decreases as the layer depth decreases, and indicates an incremental thickness variation of the hinge zone. However, the five couples of u_c and γ data still gather around the parabola forms in the u_c–γ graph (Fig. 4). The layer curves defined by the data of Table 1 are illustrated on the right lower part of Fig. 9, in which the folded area has been divided into three regions by connecting the inflection points of the layers. The gray central part with higher deformation indicates the possible oil and gas accumulation region. The curvilinear axial plane can be drawn on the map by connecting the hinge points of the folded surfaces. The geometry observed indicates that the complete description method is not appropriate in this case.

6. Discussions and conclusions

This modeling of folds is based on the use of quadratic Bézier curves, and involves joining together several segments of these curves to approximate fold shapes. In the program – Bézier Fold Profiler, a fold can be analyzed by the visual matching of the fold profile displayed on-screen from an imported digital image, which has the advantage of speed and simplicity. The results can be conveniently plotted on the u_c–γ graph in Fig. 4, where u_c and γ are respectively the axial lift-up ratio of central part and the interlimb angle.

In order to simulate complex natural folds, three more parameters, θ, T and E, were used to express the deflection angle of the axial plane, the thickness increment in the hinge zone and the limb elongation, respectively. However, it should be noted that the model does not completely represent all natural folds. Rather, a natural fold can be approximated by varying these parameters, which is convenient for quantitative analysis and comparison of folds. Further, more description parameters could be added to the model to simulate more complex fold shapes.

We have introduced two description methods to analyze the fold shape. The first method, complete fold description method, is used to analyze multiple layers. The advantage of this method is that a complete fold can be determined by thirteen parameters, which can be used in a later quantitative analysis of the fold. However, this method is not a general method, as it requires that the hinge points and deflection points are located at one straight line. Alternatively, the other method, individual layer description method, can be used to describe each individual folded layer. This method gives a more detailed description of a fold, and each folded layer is defined by seven parameters.

This paper offers a feasible way for fold classification and quantitative description. Furthermore, this method can also be used in computer modeling of folds, which is a good tool for further geometric and kinematic studies (Liu et al., 2009).

Acknowledgements

Financial support from Natural Science Foundation of China (NSFC, NO.40572119 granted to Dr. Yikun Zhang). The idea of using Bézier curves to simulate the fold arose out of discussions with Professor Zhu Guorong. We are grateful to anonymous reviewers for many valuable suggestions that notably improved the manuscript.

References

Aller, J., Bastida, F., Toimil, N.C., Bobillo-Ares, N.C., 2004. The use of conic sections for the geometrical analysis of folded profile surfaces. Tectonophysics 379, 239–254.

Bastida, F., Aller, J., Bobillo-Ares, N.C., 1999. Geometrical analysis of folded surfaces using simple functions. Journal of Structural Geology 21, 729–742.

Bastida, F., Aller, J., Bobillo-Ares, N.C., Toimil, N.C., 2005. Fold geometry: a basis for their kinematical analysis. Earth-Science Reviews 70, 129–164.

Bézier, P., 1966. Definition numérique des corbes et surfaces—I. Automatisme 11, 625–632.

Bézier, P., 1967. Definition numérique des corbes et surfaces—II. Automatisme 12, 17–21.

Chapple, W.M., 1968. A mathematical theory of finite-amplitude rock-folding. In: Geological Society of America Bulletin, vol. 79 47–68.

Coelho, S., Passchier, C., Grasemann, B., 2005. Geometric description of flanking structures. Journal of Structural Geology 27, 597–606.

De Paor, D.G., 1996. Bézier curves and geological design. In: De Paor, D.G. (Ed.), Structural Geology and Personal Computers. Pergamon Press, pp. 389–417.

Fleuty, M.J., 1964. The description of folds. In: Proceedings of the Geological Association of London, vol. 75 461–492.

Hudleston, P.J., 1973. Fold morphology and some geometrical implications of theories of fold development. Tectonophysics 16, 1–46.

Lisle, R.J., Fernández Martínez, J.L., Bobillo-Ares, N.C., Menéndez, O., Aller, J., Bastida, F., 2006. FOLD PROFILER: a MATLAB®-based program for fold shape classification. Computers and Geosciences 32, 102–108.

Liu, C., Zhang, Y., Shi, B., 2009. Geometric and kinematic modeling of detachment folds with growth strata based on Bézier curves. Journal of Structural Geology 31, 260–269.

Srivastava, D.C., Lisle, R.J., 2004. Rapid analysis fold shapes using Bézier curves. Journal of Structural Geology 26, 1553–1559.

Stabler, C.L., 1968. Simplified fourier analysis of fold shapes. Tectonophysics 6, 343–350.